

Particle Image Velocimetry and Proper Orthogonal Decomposition Applied to Aerodynamic Sound Source Region Visualization in Organ Flue Pipe

Witold MICKIEWICZ

West Pomeranian University of Technology Szczecin

Al. Piastów 17, 70-330 Szczecin, Poland; e-mail: witold.mickiewicz@zut.edu.pl

(received February 10, 2015; accepted August 31, 2015)

The paper presents experimental results of the visualization of the nonlinear aeroacoustic sound generation phenomena occurring in organ flue pipe. The phase-locked particle image velocimetry technique is applied to visualize the mixed velocity field in the transparent organ flue pipe model made from Plexiglas. Presented measurements were done using synchronization to the tone generated by the pipe itself supplied by controlled air flow with seeding particles. The time series of raw velocity field distribution images show nonlinear sound generation mechanisms: the large amplitude of deflection of the mean flue jet and vortex shedding in the region of pipe mouth. Proper Orthogonal Decomposition (POD) was then applied to the experimental data to separately visualize the mean mass flow, pulsating jet mass flow with vortices and also sound waves near the generation region as well as inside and outside of the pipe. The resulting POD spatial and temporal modes were used to approximate the acoustic velocity field behaviour at the pipe fundamental frequency. The temporal modes shapes are in a good agreement with the microphone pressure signal shape registered from a distance. Obtained decomposed spatial modes give interesting insight into sound generating region of the organ pipe and the transition area towards the pure acoustic field inside the resonance pipe. They can give qualitative and quantitative data to verify existing sound generation models used in Computational Fluid Dynamics (CFD) and Computational Aero-Acoustics (CAA).

Keywords: aeroacoustics, POD, PIV, organ flue pipe, sound field, visualization.

1. Introduction

Sound generation mechanisms in musical wind instruments are still not fully explained. The aerodynamic phenomena occurring in aerophones can be described using Navier-Stokes equation, but its solution in analytical form doesn't exist and although the computing power of existing computers has grown and the numerical simulation has developed, the simulations results can reflect real systems in only coarse way using simplified models (FABRE *et al.*, 2012). So experimental methods consisting in the velocity field measurements are still needed as a tool to understand the dynamic behaviour of air in musical instruments, where nonlinear effect of unsteady air streams is the sources of sound. Also a constant development in existing experimental methods is needed to verify the even better numerical simulations based on sound vortex theory (HOWE, 1998).

Modern measurement systems allow in-deep look at the physical phenomena due to development of new measurement sensors and sophisticated digital signal processing algorithms for measurement data processing. The mechanism of sound generation in aerophones belongs to such group of "invisibilities" which a few years ago we couldn't observe in the real conditions. Aeroacoustical phenomena observations and measurements were the background of developing the sound generation theories. As usually with experimental knowledge, the generic models have evolved. An appearance of new or improved theories, which more and more precisely reflect the behaviour of the real systems, was usually coupled with developments in the measurement technology (FLEATHER, 1976; CUADRA, 2005; PERRE *et al.*, 2012; BAMBERGER, 2005).

Observation and visualization of aeroacoustic sound generation mechanism need more sophisticated measurement technique than simple sound pressure ac-

quisition using condenser microphone. The use of traditional pressure transducer is practically impossible in hydrodynamic near field because of the big mass flow in the region of sound generation in the mouth of the organ pipe. Sound pressure level measurement from bigger distance (in medium or far field) gives an image of spatially averaged effects taking place in the organ pipe mouth. Thus, it doesn't have sufficient spatial resolution to give the opportunity to precisely reflect the dynamical phenomena in the region of interest. For such measurement objectives the anemometric techniques are more suitable, where the last main breakthrough is an introduction of non-intrusive laser measurement techniques like Laser Doppler Anemometry (LDV) and Particle Image Anemometry (PIV) (PAAL *et al.*, 2006; RAFFEL *et al.*, 2007; MOREAU *et al.* 2009). This paper is the author's contribution to the discussion of the phase-locked PIV applications (MACDONALD *et al.*, 2010; WEYNA, MICKIEWICZ, 2013; 2014).

The main difficulty in analysis of aeroacoustical field using anemometric approach is a coupled existence of an air mass flow (constant high velocity "wind") and an acoustic energy flow (smaller energy vibrating part of the flow connected with turbulences and acoustic field). To verify the existing sound generation and absorption models (ex. HOWE, 1998; YOSHIKAWA, 2013; YOSHIKAWA *et al.*, 2012) it is essential to resolve the constant and vibrating part of the flow – in the mathematical notation of the models we see separated variables describing mean mass flow ν , acoustic particle velocity u and vorticity $\omega = \text{rot } \nu$. If it is possible, the local energy transfer between mass flow and acoustic energy flow should be calculated using the formula (KOBAYASHI *et al.*, 2014):

$$\Pi_{\text{ker}} = \rho_0(\omega \times \nu) \cdot u. \quad (1)$$

To obtain ν and u separately, some researchers (YOSHIKAWA *et al.*, 2012) analyzed the interesting field using two sources of excitation: air blow for measuring mass flow parameters and pure acoustic excitation using the loudspeaker drive coupled with the pipe to observe acoustic field in the model. This approach can lead to interesting results, although in the model created on that base the mutual influence of the mass flow on the acoustic signal propagation is neglected.

In this paper another approach is proposed. The author examined the organ pipe in its normal condition – supplied with an air stream with constant velocity (two values were used). The value of time interval of PIV system was optimised for main flow parameters. The time series of raw velocity field images obtained for consecutive phases of output acoustic signal was the first information source for discussion about non-linear effects in the hydrodynamic near field of the organ pipe. For sound source identification constant velocity mass flow was separated from the variable acoustic velocity in postprocessing stage by means

of the Proper Orthogonal Decomposition (POD) and its power-dependent filtering properties. Using POD it seems to be possible to visualize only the variable in time part of the field decomposed into the orthogonal partials according to its energy. This feature of POD is called a physics filtering – different physical phenomena connected with different energy levels can be analyzed separately. The paper shows that by the use of POD it is possible to observe only that part of the field which varies in correlation to the frequency of the acoustic resonator which is the organ pipe and to the pressure signal registered in far field.

2. PIV

Particle Image Velocimetry (PIV) is a non-intrusive technique for simultaneously measuring velocity vectors field at many points in a medium flow. Starting from systems developed for fluid mechanics, the technological evolution of the last decades has extended PIV to the study of acoustic problems in air. A measurement system in which the method can be realized, needs to use interdisciplinary knowledge and technologies from areas such as electrical engineering, electronics, optics, photonics, computer technology and signal processing. Only due to the proper cooperation of these elements such a metrology system for non-electrical quantities could appear. The principle of the PIV measurement technique relies on the physical definition of velocity as a differential quotient of fluid displacement as function of time. The trajectory of many seeding particles which follow the flow constantly (it can be proved if the seeding particles have proper physical and chemical properties and adequate size) can be captured with an optical camera by illuminating a plane in the flow with two very short laser light pulses (every image in a pair seems to be still) within a time difference of a few microseconds. The particle images captured at two instants are stored in computer memory and can be processed using cross-correlation algorithms between the two pictorial distributions which are used to determine the local displacement of a restricted set of particles (RAFFEL *et al.*, 2007). Using in our case a camera with 4 megapixels resolution PIV enables the evaluation of 128×128 instantaneous velocity vectors for each image pair of the tracer particles inside the light sheet plane. Using single camera, the vectors are described in 2D by two components. Adding a second camera to the system (stereo PIV) allows evaluation of all three components of the velocity vectors in the plane of the flow field for every instant of time. An example of PIV measurement system and simple drawing of the measuring principle are shown in Fig. 4. An important feature of PIV is that a reliable basis of experimental flow field data can be obtained for direct comparison with numerical calculations and hence, for the validation of computer codes.

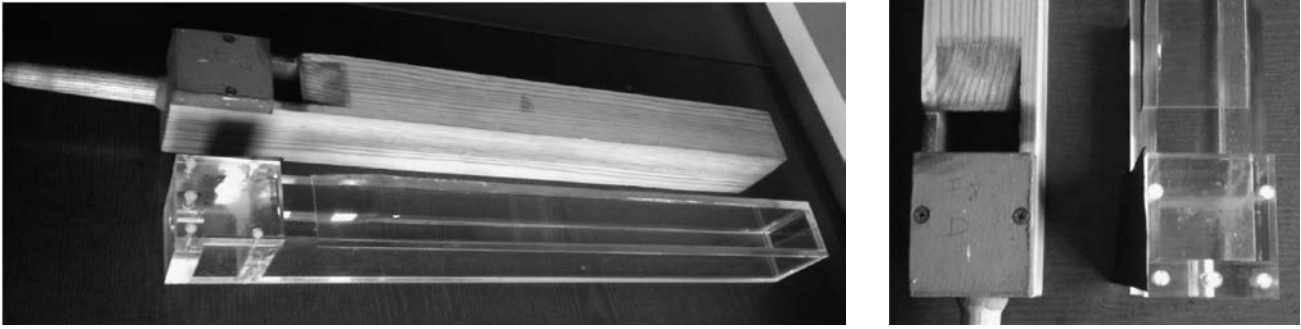


Fig. 1. The original wooden organ pipe and its transparent model (left) and the details of the pipe mouth and labium (right).

Every measurement method has its strong and weak points. In the case of PIV applied to real objects, it is usually hard to overcome the constraint that the laser light has to be introduced to the object perpendicularly to the observation plane. It is usually impossible when concerning real music instruments. To observe the phenomena in an organ pipe, using suggestions from the literature, the author built a transparent organ pipe model with the same dimensions and construction details as an original one using organic glass (Fig. 1, left). Using such a model made it possible to observe at the same time the velocity fields inside and outside of a pipe in the region of the labium (Fig. 1, right).

Geometrical details and dimensions (in mm) of the transparent model are shown in Fig. 2.

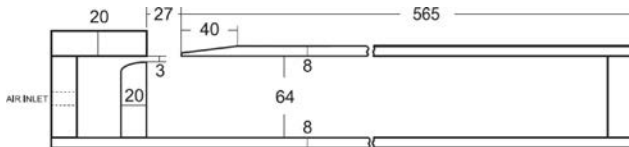


Fig. 2. Dimensions (in mm) and geometrical details of the Plexiglas pipe model.

3. Proper Orthogonal Decomposition

POD is a statistical signal processing procedure to decompose the complex velocity field into a set of the eigenfields using so called Karhunen-Loeve decomposition (LOEVE, 1955). The field synthesis based on first few most energetic components comparing to standard Fourier approach is a simpler way to produce lower-order flow field structure which contains the most significant partials of the field and can be more easily analyzed. The method is widely used in turbulent flow analysis (SIROVICH, 1987; BERKOOZ *et al.*, 1993) to obtain so called coherent structures. During the experiment we acquire the data $u(x, y, t)$, which in the case of PIV application are the instantaneous 2-D velocity vector fields (in the case presented in this paper the size of any field is 128×128 velocity vectors ($X = 128$ and $Y = 128$)). We acquire K such fields in

K instants of time. In the case of acoustical signal the snapshots should encompass at least one period of observed sound field. In our case it was one period of the pipe fundamental tone frequency and $K = 36$. These data can be transformed into the form of orthogonal temporal and spatial modes. Each temporal mode is K element vector a_k of scalar coefficients and each spatial mode is X by Y matrix with velocities. Transforming K snapshots we obtain K temporal modes and K spatial modes. Having these modes any instantaneous velocity field distribution (snapshot) $u(x, y, t)$ can be represented as a linear combination of the temporal and spatial modes:

$$u(x, y, n) = \bar{u}(x, y) + \sum_{k=1}^K a_k(n) \Psi_k(x, y), \quad (2)$$

where $\bar{u}(x, y)$ is a cycle-averaged velocity field and $a_k(n)$ is the temporal mode – the eigenvector for each spatial mode $\Psi_k(x, y)$.

To calculate POD decomposition from K snapshots we first construct the correlation matrices (one for each velocity component) according to the formula:

$$C_{ij} = \frac{1}{K} \sum_{x=1}^X \sum_{y=1}^Y u(x, y, i) u(x, y, j), \quad (3)$$

where $i, j = 1..K$ and X, Y are spatial dimensions (velocity vector number) of the analyzed field. For this matrices we find eigenvectors $a_k(n)$ and order them according to their eigenvalues λ_k . In the case of POD the calculated eigenvalues λ_k have physical meaning of energy concentrated in each mode. Their values can be used to analyze the energy spread between modes. The corresponding spatial mode $\Psi_k(x, y)$ is calculated as follows:

$$\Psi_k(x, y) = \sum_{n=1}^K u(x, y, n) a_k(n). \quad (4)$$

4. Measurement setup

The main goal of the presented research was to capture and visualize the dynamic behaviour of the air

stream in the region of labium in the transparent model of a closed organ pipe (the fundamental tone of 130 Hz) to identify the sound sources in this region. The pressure signal generated by the pipe recorded 80 cm away from the pipe labium is shown in Fig. 3.

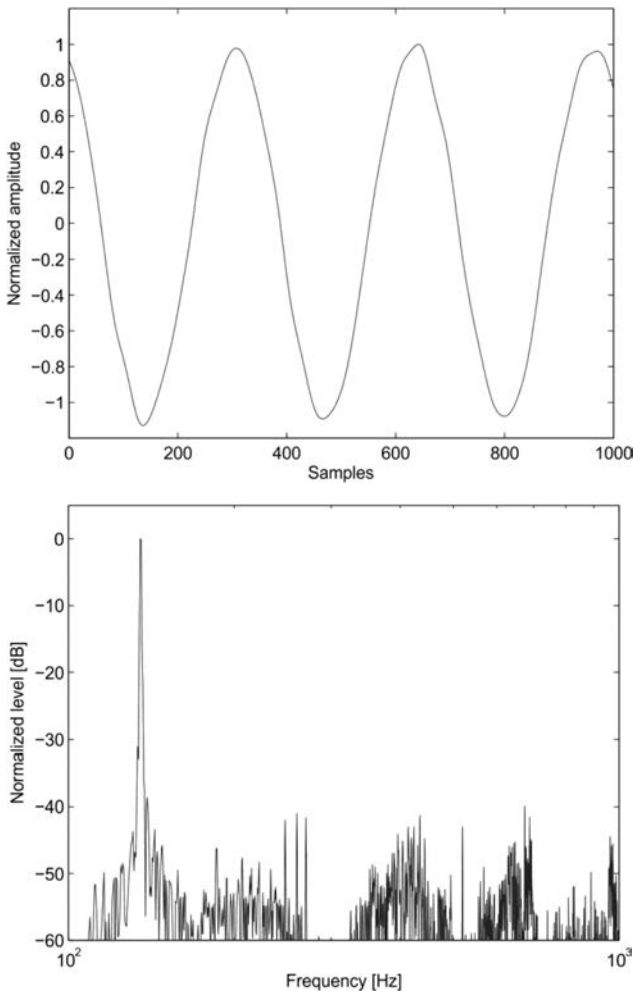


Fig. 3. The pressure signal generated by the pipe in time (top) and frequency (bottom) domains with normalized amplitudes.

The pictures of velocity fields were obtained using a planar phase-locked PIV technique. The data acquisition was synchronized to the pressure signal of the tone generated by the pipe itself captured by the microphone located near the mouth. The measurement setup diagram is shown in Fig. 4. The experimental stand is based on the PIV system delivered by LaVision GmbH Goettingen Germany. It consists of the Litron laser model Nano TRL 325-15 as a light source. The images are acquired by a digital 4-megapixel CCD camera (LaVision Imager Pro X 4M) with the resolution of 2048×2048 pixels. During the experiments the camera was connected to a PC equipped with a frame grabber (Matrox Solios eCL CameraLink) that received 14 bit images at a rate of 15 Hz (7 Hz rate for image pairs). LaVision Programmable Synchronisation Unit

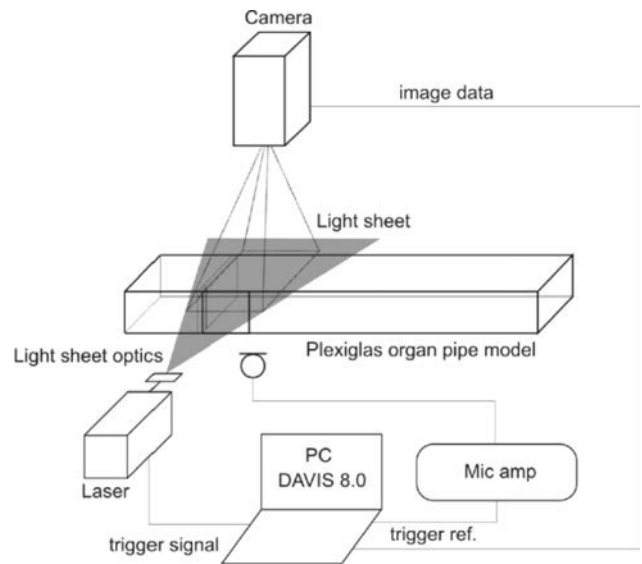


Fig. 4. Schematic diagram of the experimental stand.

was used to control the timing of the laser pulses and synchronize the acquisition. The acoustic signal generated by the pipe and received by the condenser microphone Microtech Gefell MK102 was amplified and supplied to synchronisation unit input.

The blower was used to supply the air to the pipe. During experiments two values of input air velocity were used. The air was mixed with a seeding particles (droplets of $1 \mu\text{m}$ in diameter of Di-Ethyl-Hexyl-Sebacat oil with density of 912 kg m^{-3}) generated in the LaVision aerosol generator. The instantaneous velocity fields were calculated from the collected seeding particles image pairs using DaVis 8 software. The computational algorithm used interrogation area of 32×32 pixels with 50% overlap. As a calculation result a vector field of 128×128 velocity vectors (about 1 vector per 1 mm^2 of the field of view) was obtained for each acquisition phase. This vector field is a result of averaging the 50 instantaneous fields recorded for the same phase. This fact is crucial for POD analysis because by doing that we can record the variation of the field which is correlated to the acoustics, and remove (average) the turbulence effects connected with incompressible main mass flow. Each velocity vector was described by two orthogonal velocity components. Before experiments the calibration procedure of optical system was performed using calibration plate supplied with the system. The procedure was applied according to steps provided by DaVis software. The accuracy of seeding particle displacement is of about 0.17 pixel with the pixel size of $7.4 \mu\text{m}$. It gives displacement accuracy of $1.3 \mu\text{m}$. The accuracy of velocity evaluation depends on time interval Δt . The maximum value of velocity in observed region was about 16 m/s. To properly observe in such conditions the seeding particles shift, what is the base for velocity calculation, the time interval Δt was set to $30 \mu\text{s}$.

5. Results

All velocity fields presented in the paper were recorded in the plane of the pipe symmetry perpendicular to the organ pipe mouth. On the following figures pipe walls are shown with white colour. The green areas without data are the places of strong light reflections from Plexiglas boundaries which had to be shielded to avoid a damage of the digital camera image sensor. In the preliminary step the visualization of the vibrating air stream in the original organ pipe was done. Due to wooden walls of the pipe the field can be observed only outside the labium. The wooden pipe generated the sound with fundamental tone of 128 Hz. The acquisition of pictures in phase-locked PIV system was synchronized to 20 phases of one 128 Hz cycle. So the flow field was sampled with 2560 S/s rate (sampling interval 390 μ s). From the sampling theory point of view, the 9 harmonics can be taken into consideration without the aliasing effect. The amplitude systematic error for higher frequencies could be corrected according to (MICKIEWICZ, 2014b). The field of observation in relation to the rest of the pipe and the examples of instantaneous velocity fields for phases 4, 9 and 18 are shown in the Fig. 5. We can observe the main air stream exiting the flue. The trajectory of the

stream evolves (vibrates) and one big moving vortex below the stream is seen. The flow stays turbulent far away from the labium.

Using the transparent model we can observe the relation between the field inside and outside of the pipe. The evolution of the flow field over one period of fundamental tone was acquired at 36 equidistant phases per one period (MICKIEWICZ, 2014a). In Fig. 6 we can see the complex flow in the chosen phases and the orientation of the presented field in relation to the pipe. We can easily notice the vibrations of the main air stream exiting the flue and moving vortices of both sides of the air stream. The time series of raw velocity field distribution images show nonlinear sound generation mechanisms: the large amplitude of deflection of the mean flue jet and vortex shedding in the region of pipe mouth. The turbulent flow evolves in different ways outside and inside the pipe. The turbulent region is faster organized in linear acoustic field inside the pipe than outside. It is the influence of resonating properties of the closed pipe and existing here standing waves.

To compare a measurement data with existing models in qualitative and quantitative way it is necessary to distinguish in these field visualizations the pure vibrating (acoustic) energy. This problem has been

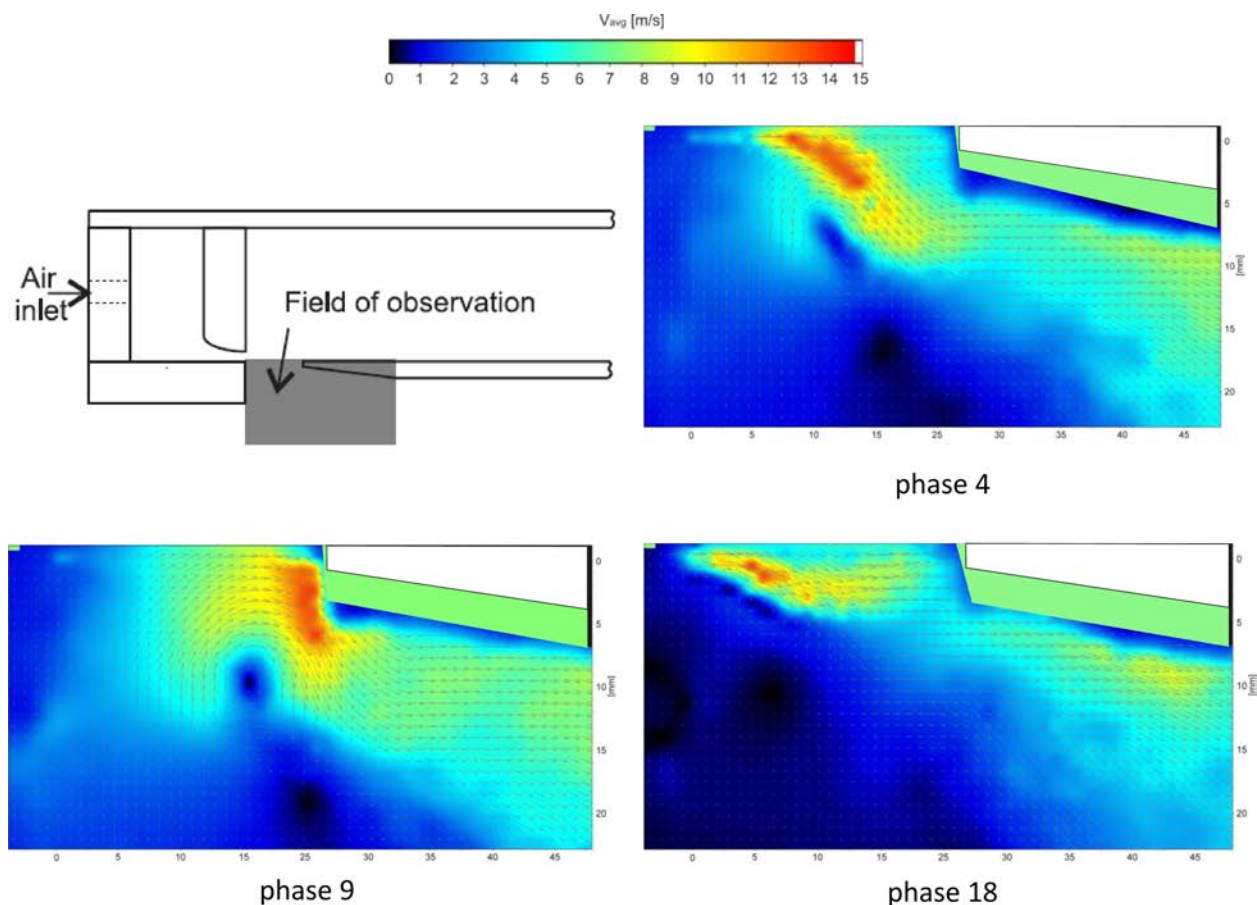


Fig. 5. Flow field evolution in chosen phases in the original organ pipe.

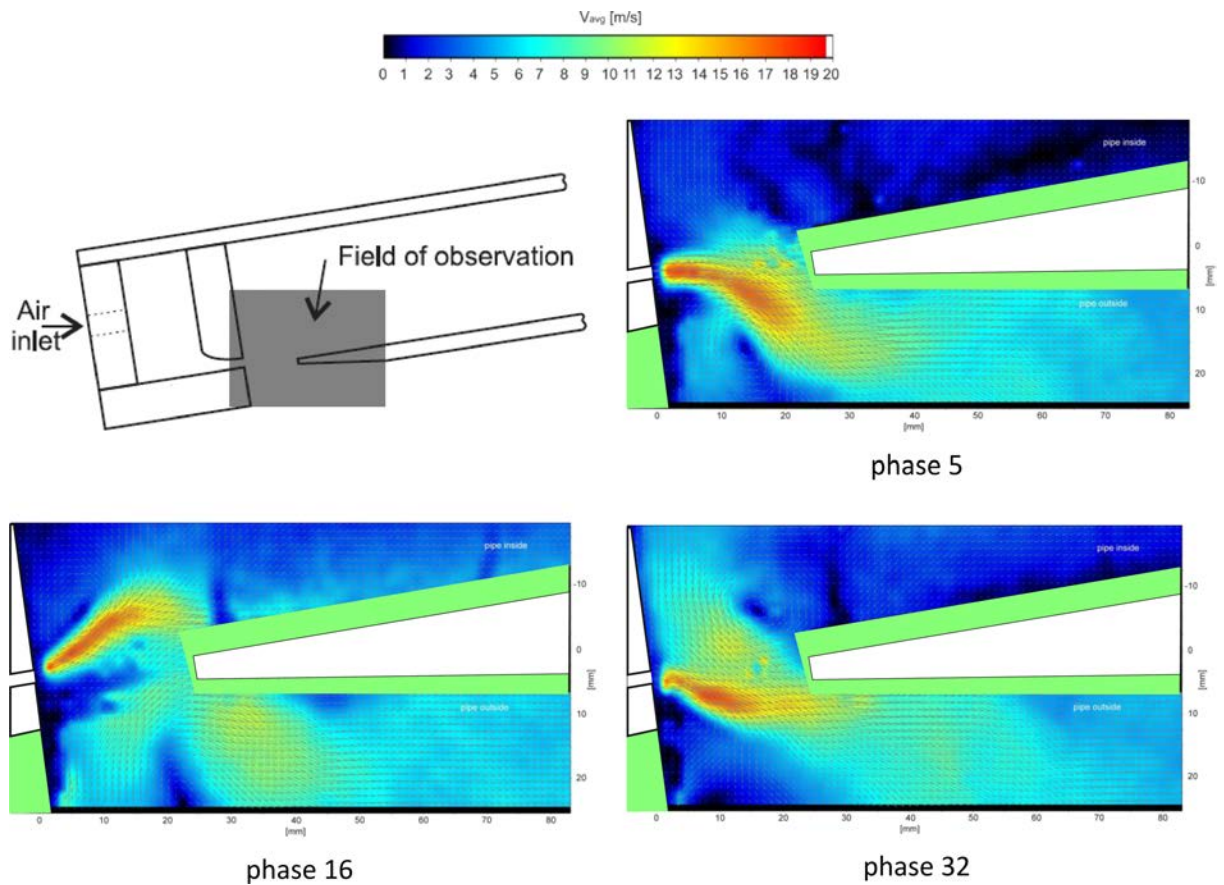


Fig. 6. Flow field evolution in chosen phases in the transparent Plexiglas pipe model.

approached by different researchers in many ways but they usually used different excitation sources for observing complete flow and pure acoustic flow. For example in (YOSHIKAWA *et al.*, 2012; YOSHIKAWA, 2013) to measure the whole turbulent mass flow the blower was used and for acoustic flow only observations the loudspeaker driver was coupled with the pipe. In this paper another approach is used. The image series of time evolution of the velocity fields were then used

as the snapshots for POD analysis. Using POD analysis the mixed aeroacoustic flow was separated into constant in time mean mass flow and the set of spatial modes representing vibrating part of the flow. As mentioned before each spatial mode coexists with the temporal mode (eigenvector).

In Fig. 7 the mean averaged mass flow is shown for two different inlet air velocities. This velocity field representation gives the information about v quantity

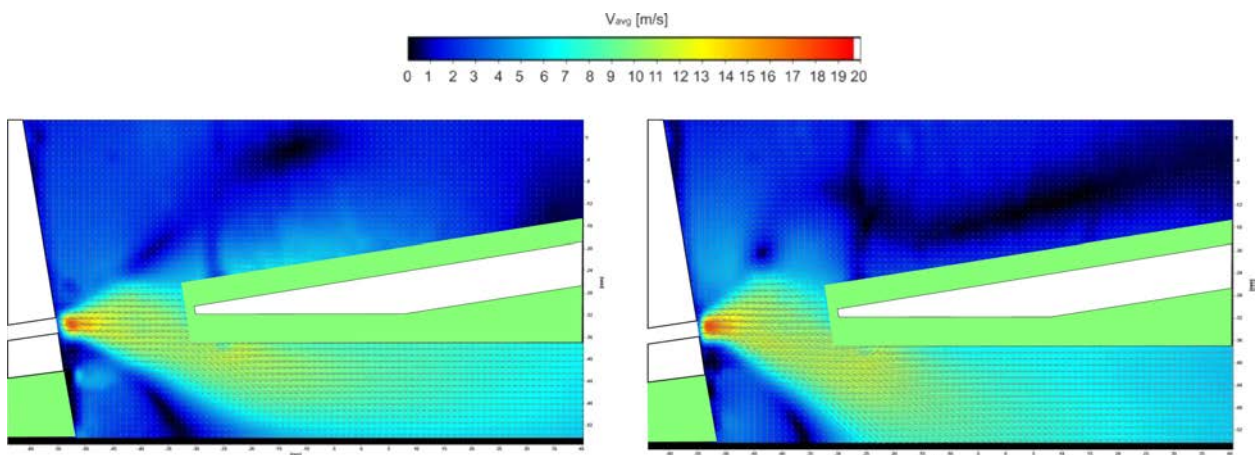


Fig. 7. Mean flow velocity field at 13 m/s (left) and 16 m/s (right).

in Eq. (1). Some general parameters of the mean flow fields are presented in the Table 1.

Table 1. Parameters of the mean mass flow.

| Velocity [m/s] | Case 1 | Case 2 |
|----------------|---------------|---------------|
| V_{xMAX} | 16.0 | 13.4 |
| V_y | -4.76 : +3.75 | -3.17 : +3.98 |
| $ V _{MAX}$ | 16.005 | 13.42 |

By subtracting the constant (mean) part of the flow from the whole flow field we can focus only on vibrating part. The organ pipe being under investigation produces the sound with the 128 Hz fundamental tone. The microphone signal oscilogram matches sinusoid at lower air inlet velocity and is more complex (contains more overtones) for higher air inlet velocity. Using POD we can have better insight into flow dynamics connected with consecutive power density levels. As it was mentioned before, eigenvalues of correlation matrices have the physical meaning of energy. In the case of 2-D analysis we dispose two sets of eigenvalues λ_x for correlation matrix of x -direction velocity spatial components and λ_y for correlation matrix of y -direction velocity spatial components. So the energy content in i -th spatial mode in percents can be calculated as follows:

$$\text{Energy Content}(i) = \frac{\lambda_x(i) + \lambda_y(i)}{\sum_{k=1}^K (\lambda_x(k) + \lambda_y(k))} \cdot 100\%. \quad (5)$$

The sum of energies contained in first n modes can be calculated as:

$$\text{Sum of energies}(n) = \sum_{i=1}^n \text{Energy Content}(i). \quad (6)$$

In the case of music instruments energy spread is correlated with the harmonics content. As we know, POD is rather statistical decomposition method, but in the case of the organ pipe sounds first modes quite well correspond to first overtones and next represent more noise content. In Fig. 8 we can see the energy distribution in consecutive modes.

As we can see, in the first case (higher air speed, solid lines) over 95% of energy contains first 4 modes, what corresponds to first two harmonics. In this case the pipe tone is well established and harmonic part dominates over noise part. In the second case (lower air speed) the pipe is undersupplied with air and higher modes contain more energy in reference to fundamental tone – the timbre of the pipe is different and more noises are audible. Because we observe the acoustic waves which propagate, with the consecutive harmonics correspond two spatial and temporal modes. In

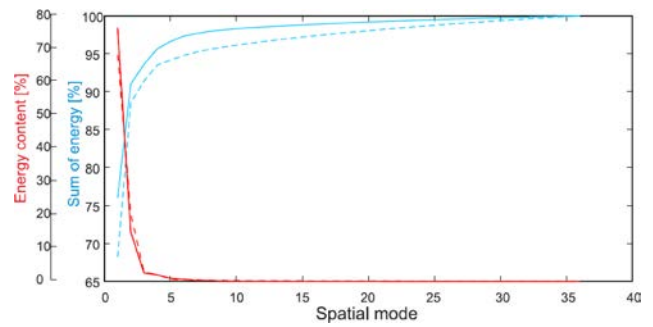


Fig. 8. Vibrating energy distribution in POD modes for two air inlet velocity cases.

Fig. 9 we can see the first two spatial modes. They correspond to the fundamental tone of 128 Hz.

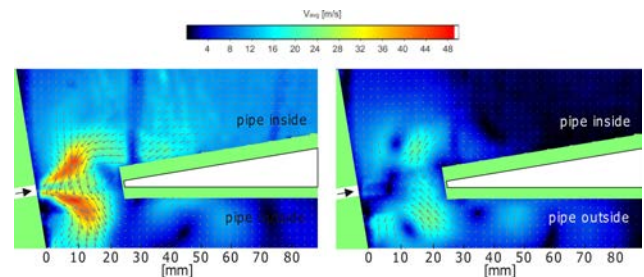


Fig. 9. First two spatial modes of the vibrating part of the flow in case 1.

Temporal coefficients with the same frequency are shifted by 90 degrees. Perfect cosinusoidal coefficients and measured values are shown in Fig. 10.

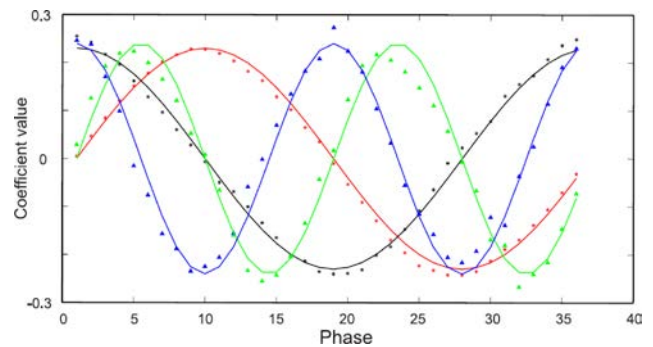


Fig. 10. POD first 4 temporal modes (coefficients $a_k(n)$ in Eq. (2)) of measured data (stars and triangles) and perfect cosinusoidal harmonic components shifted in pairs by 90 degrees.

Combination of two first spatial and temporal modes of the blown pipe shown in Figs. 9 and 10 can be interpreted as a generic organ pipe sound source with the fundamental frequency and used in formula (1) as variable u . Its time evolution is shown in Fig. 11.

As we can see, even fundamental tone of the organ pipe is generated by the source, which is quite complex comparing to perfect point or dipole source. An in-

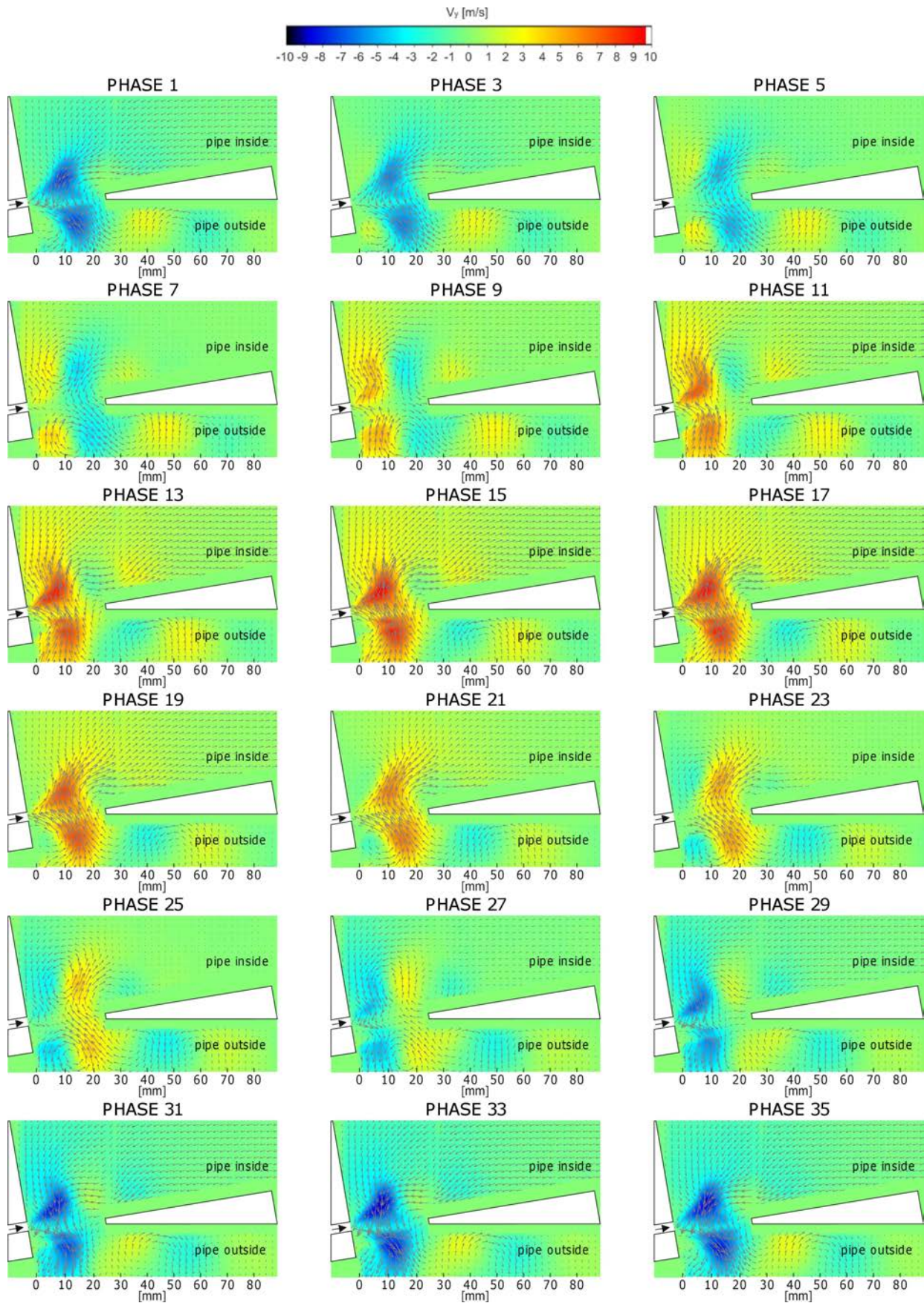


Fig. 11. The two POD modes approximation of an acoustic velocity field evolution in transparent pipe model (fundamental frequency of 128 Hz, one period divided into 36 equidistant phases, every second phase is shown).

interesting phenomenon can be observed in phases 5–9 and 23–28 where the air movement in the pipe mouth has partially opposite directions due to a big vortex formation of both sides of the mean flow. In equilibrium (phases 7 and 25) we can see still high velocities in mouth region, but in the standing waves region the acoustic velocity is near zero. It is very important point. When we need to analyse the sound propagation and far sound field distribution using some computational aeroacoustics algorithms, the results can be ambiguous due to the wrong assumptions concerning sound source properties.

6. Discussion and conclusion

The phase-locked particle image velocimetry is very useful method to study aeroacoustical velocity fields in organ pipes. The application of the transparent Plexiglas organ pipe model allowed to study in the same time velocity field evolution outside and inside a blown organ pipe labium. The image acquisition synchronized directly to the sound generated by the pipe allows to obtain highly time resolved picture of dynamic evolution of the air jet in the region of organ pipe labium. The time resolution is in this case not a function of the sampling rate of the system but the total acquisition time and the possibility to maintain the stable working conditions during the experiment. In the transparent model it is easy to see the transition area from aerodynamic to pure acoustic field inside the pipe resonator. The application of Proper Orthogonal Decomposition gives new opportunities to decompose the velocity field in constant and vibrating field components. Further research and discussion have to be devoted to the possibility of distinguishing in this way the compressible and incompressible behaviour of the observed variable field. Analysing the time varying field components correlated with the generated sound frequency can be used to build a more realistic model of organ pipe as a complex sound source.

Acknowledgments

The author likes to express his gratitude to prof. Stefan Weyna for his scientific support and for unconstrained access to his Image Laser Anemometry Laboratory at the Faculty of Maritime Technology and Transport of West Pomeranian University of Technology in Szczecin, Poland.

References

1. BAMBERGER A. (2005), *Vortex sound in flutes using flow determination with endo-piv*, 4th European Congress on Acoustics (Budapest), 665–70.
2. BERKOOZ G., HOLMES P., LUMLEY J.L. (1993), *The proper orthogonal decomposition in the analysis of turbulent flows*, *Annu. Rev. Fluid Mech.*, **25**, 539–575.
3. CUADRA P. (2005), *The sound of oscillating air jets: physics, modelling and simulation in flute-like instruments*, PhD thesis, Stanford University.
4. FABRE B., GILBERT J., HIRSCHBERG A., PELORSON X. (2012), *Aeroacoustics of Musical Instruments*, *Annu. Rev. Fluid Mech.*, **44**, 1–25.
5. FLETHER N.H. (1976), *Transients in the speech of organ flue pipes – a theoretical study*, *Acustica*, **34**, 224–233.
6. HOWE M.S. (1998), *Acoustics of Fluid-Structure Interactions*, Cambridge University Press.
7. KOBAYASHI T., AKAMURA T., NAGAO Y., IWASAKI T., NAKANO K., TAKAHASHI K., AOYAGI M. (2014), *Interaction between compressible fluid and sound in a flue instrument*, *Fluid Dyn. Res.*, **46**, 061411 (14 pp).
8. LOEVE M. (1955), *Probability theory*, D. Van Nostrand, New York.
9. MACDONALD R., SKULINA D.J., CAMPBELL D.M., VALIERE J.-CH., MARX D., BAILLIERT H. (2010), *PIV and POD Applied to High Amplitude Acoustic Flow at a Tube Termination*, Proceedings of 10-eme Congres Francais d’Acoustique, Lyon.
10. MICKIEWICZ W. (2014a), *Visualization of sound generation mechanism in organ flue pipe by means of particle image velocimetry*, Proc. of 7th Forum Acusticum, Kraków, Poland.
11. MICKIEWICZ W. (2014b), *Systematic error of acoustic particle image velocimetry and its correction*, *Metrolology and Measurement Systems*, **21**, 3, 447–460.
12. MOREAU S., BAILLIET H., VALIERE J.-CH., BOUCHERON R., POIGNAND G. (2009), *Development of Laser Techniques for Acoustic Boundary Layer Measurements, Part II: Comparison of LDV and PIV Measurements to Analytical Calculations*, *Acta Acustica united with Acustica*, **95**, 805–813.
13. PAAL G., ANGSTER J., GAREN W., MIKLOS A. (2006), *A combined LDA and flow-visualization study on flue organ pipes*, *Experiments in Fluids*, **40**, 825–835.
14. PERRE G., NILA A., VANLANDUIT S. (2012), *Measurement of sound and flow fields in an organ pipe using a scanning laser Doppler vibrometer*, 16th Int Symp on Applications of Laser Techniques to Fluid Mechanics, Lisbon.
15. RAFFEL M., WILLERT C., KOMPENHANS J. (2007), *Particle image velocimetry: a practical guide*, Springer, Berlin, New York, Heidelberg.
16. SIROVICH L. (1987), *Turbulence and the dynamics of coherent structures. Part 1: Coherent structures*, *Quarterly of App. Math.*, **45**, 561–571.
17. WEYNA S., MICKIEWICZ W. (2014), *Phase-Locked Particle Image Velocimetry Visualization of the Sound*

- Field at the Outlet of a Circular Tube*, Acta Physica Polonica A, **125**, 4-A, A-108–112.
18. WEYNA S., MICKIEWICZ W. (2013), *Experimental acoustic flow analysis inside a section of an acoustic waveguide*, Archives of Acoustics, **38**, 2, 211–216.
19. WEYNA S., MICKIEWICZ W. (2014), *Multi-Modal Acoustic Flow Decomposition Examined in a Hard Walled Cylindrical Duct*, Archives of Acoustics, **39**, 2, 289–296.
20. YOSHIKAWA S., TASHIRO H., SAKAMOTO Y. (2012), *Experimental examination of vortex-sound generation in an organ pipe: A proposal of jet vortex-layer formation model*, Journal of Sound and Vibration, **331**, 11, 2558–2577.
21. YOSHIKAWA S. (2013), *Aerodynamical sounding mechanism in flue instruments: Acceleration unbalance between the jet vortex layers*, ICA 2013, Montreal in Proc. of Meetings on Acoustics, 19, 1–9.